

Single-dot spectroscopy of CdS nanocrystals and CdS/HgS heterostructures

Felix Koberling, Alf Mews,* and Thomas Basché
Institut fuer Physikalische Chemie, Welderweg 11, 55099 Mainz, Germany
(Received 24 December 1998)

The low-temperature fluorescence of single CdS nanocrystals and of single CdS/HgS/CdS quantum well quantum dots (QDQW's) where an atomic monolayer of HgS is embedded in a CdS nanocrystal is compared. The fluorescence spectrum of the CdS nanocrystals depends strongly on the laser excitation intensity. At high excitation intensity several fluorescence lines can be detected. The total fluorescence intensity of the CdS particles is fluctuating and can be interrupted by dark periods as long as seconds. The spectral and intensity fluctuations are strongly reduced for the QDQW's which can be explained by charge carrier localization in the HgS region of the nanocrystals. At lowest excitation intensity the linewidth can be narrowed down to sub meV. [S0163-1829(99)03027-1]

I. INTRODUCTION

Colloidal semiconductor nanocrystals with dimensions smaller than the bulk exciton show unique optical properties which depend strongly on the size.^{1,2} The change of the electronic level structure can be explained by the strong confinement of the charge carriers in all three dimensions. Recently, multiband effective mass approximations have been developed to explain the size-dependent absorption spectra of II-VI (Ref. 3) and III-V (Ref. 4) semiconductor nanocrystals in great detail.⁵

Besides the size quantization, surface effects are also known to influence the optical properties of these nanometer particles. It has been shown recently that especially the fluorescence emission of the nanocrystals is sensitive to the presence of defects which might arise because not all of the dangling bonds on the particle surface can be saturated by molecular ligands.⁶ For example it was proposed that the low fluorescence quantum yield of approximately 10% was due to radiationless recombination centers on the surface.⁷ To suppress surface effects, inorganic passivation has been utilized where the nanocrystals have been covered with a high band gap material.⁸⁻¹⁰ It could be shown that the fluorescence quantum yield was increased dramatically because all the atoms of the "active core" were in a well ordered crystallographic environment.

Parallel to the core-shell particles a nanocrystal system has been developed, in which only a layer of a low band gap material (HgS) is spherically embedded in a CdS nanocrystal leading to a quantum well within a quantum dot (QDQW).¹¹ In these particles the photoexcited charge carriers are expected to be mainly localized within the HgS well¹² which should have a pronounced effect on the optical properties of the particles.

By employing appropriate microscopic techniques it recently became feasible to image the fluorescence of single semiconductor nanocrystals.¹³⁻¹⁷ These experiments demonstrated the importance of single dot luminescence studies for an increased understanding of optical interactions in semiconductor nanocrystals. Effects such as blinking of the fluorescence emission¹³ or spectral shifts of the luminescence lines^{15,17} have been reported. The line shifts which reached

values of more than 50 meV were explained by a randomly changing excited state dipole built up by electronic charge carriers in different surface traps.¹⁷ As these shifts were not only observed in bare nanocrystals but also in core-shell structures, there is obviously still a probability for the charge carriers to get trapped on surface sites as the thickness of the passivating layer is only a few atomic monolayers. Additionally, the spontaneous spectral diffusion caused by charge carriers in surface traps is still on the same order of magnitude as for uncoated nanocrystals because the polarizability of the inner core is still the same as in bare particles.

In this work we compare the single dot luminescence spectra of bare CdS nanocrystals with those of CdS/HgS/CdS nanocrystals. In the QDQW's the reduced polarizability is expected to influence the spectral diffusion of the luminescence line. We show that the spectra change dramatically upon embedding just a single monolayer of HgS into a CdS quantum dot even though the stoichiometric fraction of the HgS is only 15%. The results suggest that the charge carriers can indeed be locally confined within a quantum dot by building up complex nanocrystals of different materials.

II. EXPERIMENTAL

The synthesis of the CdS particles and the CdS/HgS QDQW's has been described in detail elsewhere.¹⁸ Briefly it starts with the preparation of the CdS cores in an aqueous solution by addition of H₂S gas to a dissolved cadmium salt in the presence of hexametaphosphate (HMP) which serves as an inorganic molecular ligand. The reaction is carried out in a 2 l flask equipped with a septum, pH meter, and a gas inlet to purge the ultra pure water with argon before the reaction takes place. First 2×10^{-4} mol/l cadmium perchlorate and the same amount of HMP are dissolved in 2 l of water and than the pH is adjusted to a value of 9.4. The injection of 9 ml H₂S gas leads to a rapid nucleation of CdS clusters which grow in the next 10 min to almost uniform size of approximately $5 (\pm 1)$ nm in diameter. An emission and absorption spectrum of the colloidal CdS solution is shown in Fig. 1. In the next step the surface of the particles is modified by addition of dissolved mercury ions which replace the surface cadmium ions thus forming a monolayer of

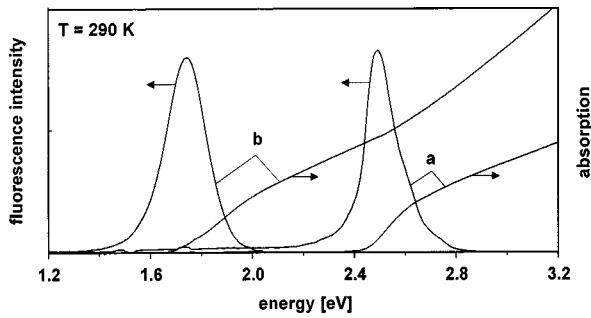


FIG. 1. Ensemble absorption and emission spectra of CdS particles (a) with a diameter of $5 (\pm 1)$ nm and of CdS/HgS/CdS QDQW's [(b) diameter: $6.5 (\pm 1)$ nm]. The absorption onset and the emission frequency shift by almost 1 eV upon embedding a single atomic monolayer of HgS into the CdS nanocrystals.

HgS because the solubility of HgS is much lower than that of CdS. Finally the surface is covered with CdS by growing additional CdS on top of the HgS thus forming the final QDQW's. From Fig. 1 it can be seen that the absorption edge and the emission is shifted to lower energies upon embedding a single layer of HgS.

The particles were dispersed on a quartz cover slip and mounted on a piezoscanner of a low-temperature confocal microscope¹⁹ with a scan range of $5 \times 5 \mu\text{m}^2$ at 10 K. In the confocal geometry the excitation and detection volume are determined by a diffraction limited spot size (diameter $\approx \lambda/2$) and therefore the background fluorescence from the substrate and interfering fluorescence from further nanocrystals in the vicinity of the one investigated is strongly suppressed. In addition this geometry allows us to record single dot emission spectra with varying excitation intensities up to 50 kW/cm^2 by directing the fluorescence light to a spectrometer equipped with a liquid-nitrogen-cooled charge-coupled device (CCD) camera.

In the first step of the experiment the sample is scanned through the excitation spot and the total fluorescence is detected with an EG&G avalanche photodiode (APD) to record a fluorescence image. Figure 2 (left) shows a fluorescence image of isolated CdS particles where the laser intensity for excitation at $\lambda = 442 \text{ nm}$ was 1.5 kW/cm^2 . The picture consists of 128×128 pixels and the integration time per pixel is 10 ms. The upper spectrum in Fig. 2 (right) shows the integrated emission spectrum while scanning, which is recorded simultaneously with picture 2 (left) by using a beam splitter and directing 42% of the fluorescence light to the APD and 55% to the spectrometer. In this way it is also possible to record the integrated fluorescence of a single particle as a function of time (fluorescence time trace) and the corresponding spectra at the same time. The two lower spectra in Fig. 2 (right) which stem from the two isolated nanocrystals marked in Fig. 2 (left) were recorded with an excitation intensity of 0.25 kW/cm^2 for 20 s each.

III. EMISSION OF SINGLE CdS NANOCRYSTALS

On the right side of Fig. 3 emission spectra of a single CdS nanocrystal at different excitation intensities at 20 K are shown ($\lambda_{\text{exc}} = 442 \text{ nm}$). At low excitation intensity a single emission line can be detected whereas several additional lines appear at higher intensities. One might argue that at high excitation intensity the multiplet of lines is due to emission of nanocrystals excited in the wings of the excitation profile. We can rule out this possibility because the sum of spectra from the potentially accessible emitters in the vicinity of a given nanocrystal does never correspond to the spectrum of this nanocrystal at high excitation intensity.

In addition to the spectral changes upon variation of excitation intensity, the total fluorescence intensity fluctuates as well. On the left hand side of Fig. 3 fluorescence time traces and the corresponding spectra for different detection time windows are shown. At lowest excitation intensity the fluo-

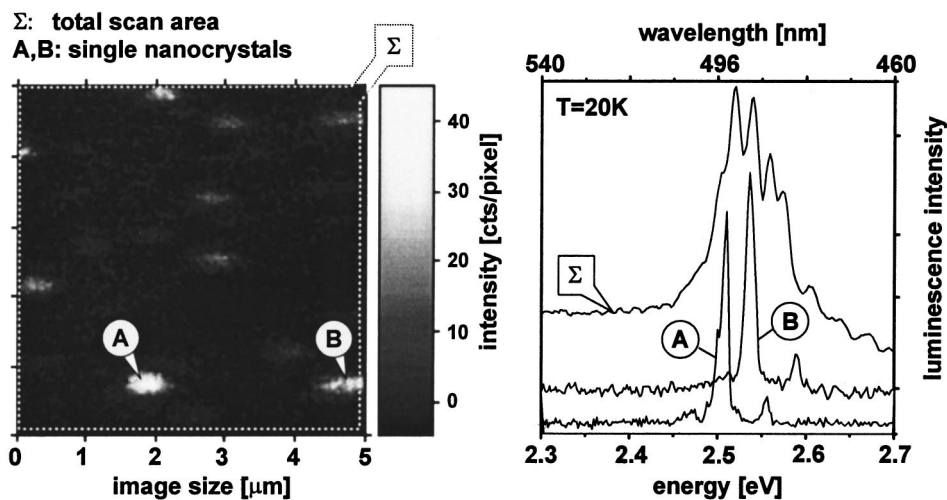


FIG. 2. Spatial selection of single CdS nanocrystals on a quartz cover slip. The picture on the left shows a fluorescence image of isolated CdS nanocrystals recorded via scanning in a low-temperature confocal microscope ($T = 20 \text{ K}$). The total fluorescence was excited at 442 nm and detected with an EG&G/APD. The picture consists of 128×128 pixels (dwell time: 10 ms/pixel); the excitation intensity while scanning was 1.5 kW/cm^2 . 55% of the fluorescence light was directed to a spectrometer during the scanning process resulting in the Σ spectrum on the right. The spectra A and B were taken after moving the scanner to the bright spots marked in the fluorescence image. The excitation intensity was adjusted to 0.25 kW/cm^2 and the acquisition time was 20 s. At these conditions a second emission line can be seen in both spectra which is shifted by 5 meV to the blue of the main peak.

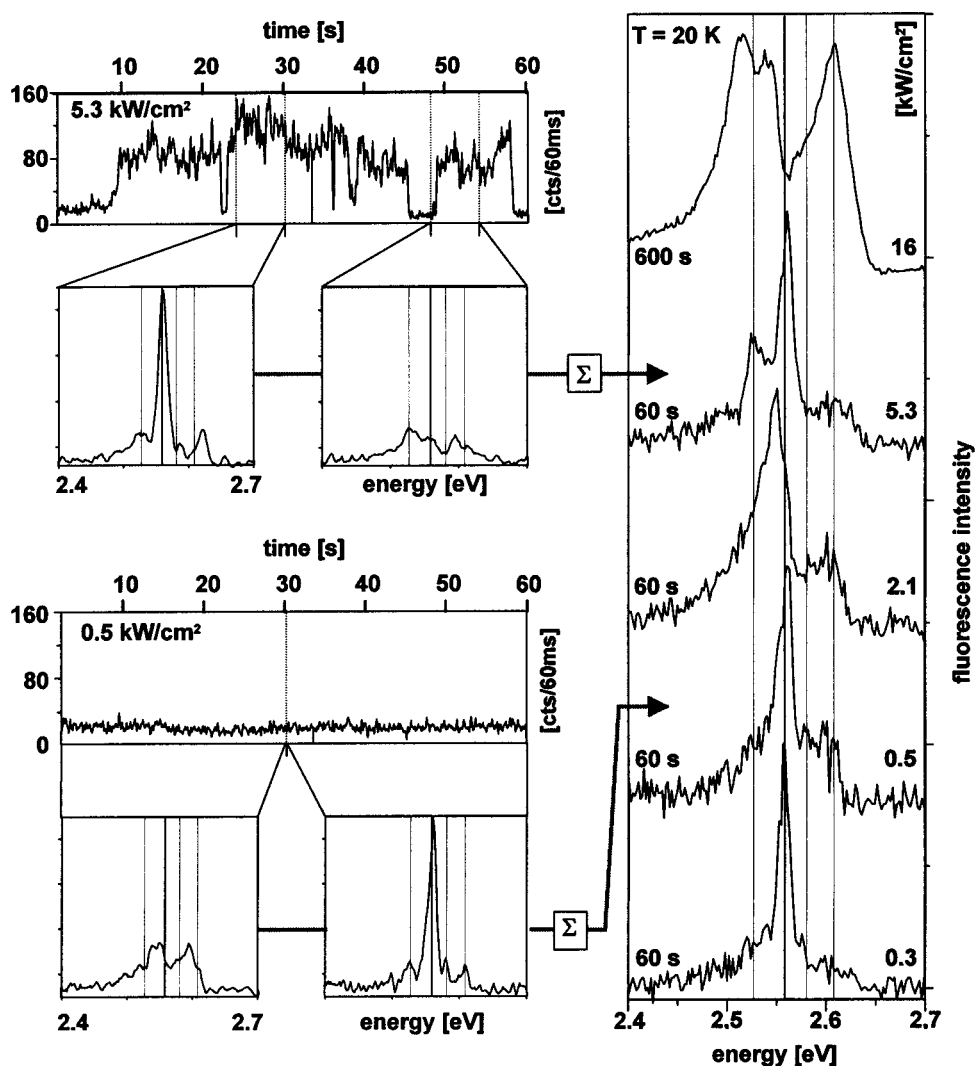


FIG. 3. Evolution of the emission spectra of single CdS nanocrystals at different excitation intensities ($T=20$ K, $\lambda_{\text{ex}}=442$ nm). On the right-hand side it can be seen that several spectral lines appear at higher excitation intensity. In order to compare the time-dependent fluorescence intensity with the spectra, part of the light (42%) was directed to the APD while taking the spectra. The results on the left show that the total fluorescence only fluctuates at irradiation intensities above 1 kW/cm^2 . At very high power the particle emission sometimes turns ‘‘off’’ for several seconds before it stops completely. Additionally, fluorescence spectra for several time periods were taken. The spectra on the bottom (left) show that there is no direct correlation between the total fluorescence intensity and the intensity distribution between the various fluorescence lines.

rescence intensity is almost constant in time whereas at higher laser power the fluorescence can be interrupted by dark periods as long as seconds. Additionally, it can be seen that intensity fluctuations between the different emission lines cannot be directly correlated with the corresponding time trace. For example, at an excitation intensity of 0.5 kW/cm^2 the fluorescence time trace shows almost no fluctuation whereas the intensity distribution between the different emission lines fluctuates dramatically.

The origin of the different spectral lines is not clear yet. Empedocles and Bawendi performed fluorescence measurements on single CdSe nanocrystals which showed that the spectral position can undergo spontaneous shifts in the range of 75 meV .¹⁷ This ‘‘spectral diffusion’’ was attributed to charge carriers trapped in various surface states of the particle. Depending on the actual trapping geometry these charges polarize the excited state differently thus shifting the luminescence lines in the same way as an applied external

electric field (Stark effect). The spacing between the various spectral positions of the CdS nanocrystals investigated in this work is on the same order of magnitude suggesting that trapped charge carriers might also be responsible for the spectral fluctuations. On the other hand, the spectral positions of the single CdS particles do not shift continuously as can be seen from Fig. 3. At high excitation intensity there is still some structure discernible in the spectra. Actually, under these conditions any spectrum of the 10 nanocrystals which have been investigated in all detail can be fitted reasonably with four distinct peak positions.

The distinct spectral positions might be due to distinct surface trap sites of the CdS particles which are not spherical in shape. From TEM measurements it was shown that zinc-blende-type CdS particles can be described as truncated tetrahedra where the 111 surfaces are eventually formed by cadmium cations.²⁰ The truncated corners would then be sulfur rich and could serve as distinct hole traps. By arranging

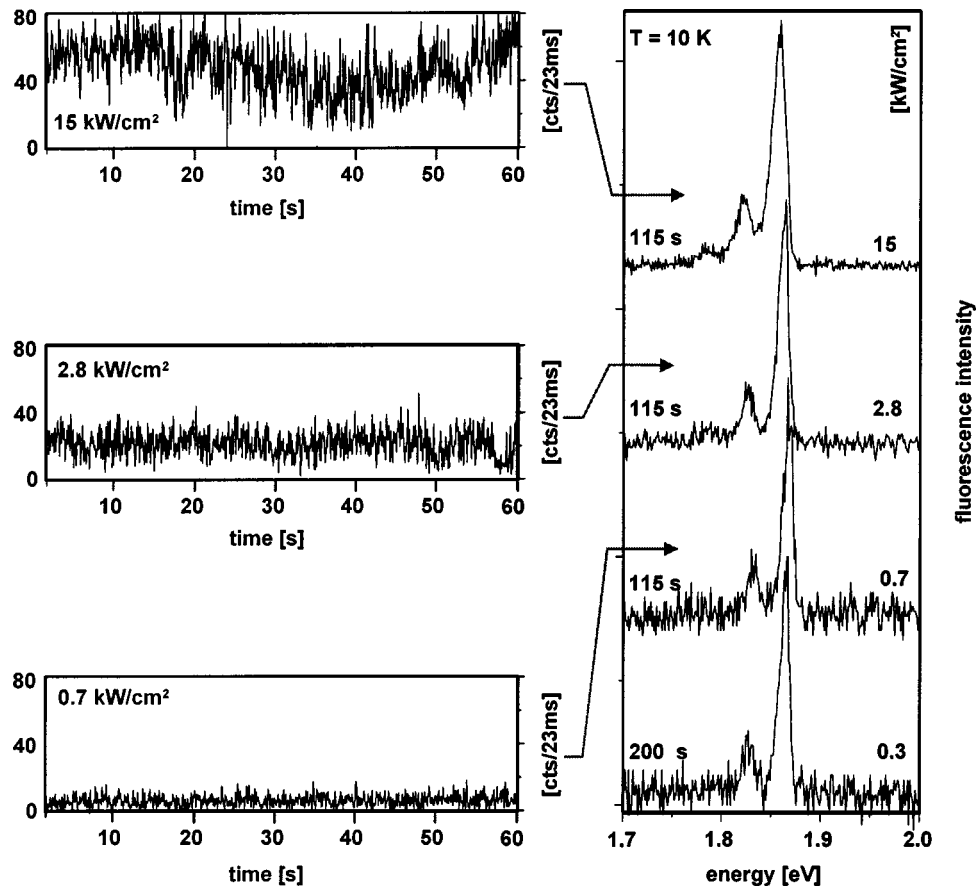


FIG. 4. Fluorescence spectra and fluorescence time traces of CsS/HgS/CdS QDQW's at different excitation intensities ($T=10$ K, $\lambda_{\text{ex}}=633$ nm). Compared to the CdS spectra in Fig. 3 the QDQW's show much less intensity fluctuations and a single fluorescence line with phonon replicas to the low-energy side can be observed at any excitation intensity. The phonon frequency is 285 ± 5 cm^{-1} and the coupling (Huang-Rhys) parameter is 0.25 ± 0.05 .

the charge carriers in the appropriate trap sites electric fields may be created that lead to certain transition frequencies. In a first estimate we calculated the effect of point charges on opposite sites of a CdS tetrahedron on the transition frequencies. The field strength of two point charges separated by a distance r (50 Å) is of the order of $\zeta = 5 \times 10^7$ V/cm where we used a value of $\epsilon = 10$ for the dielectric response of the CdS nanocrystal. If we assume that the excited state is delocalized over the whole particle, i.e., the polarizability volume α is in the range of 5×10^5 Å³, the frequency shift $\Delta E = \frac{1}{2} \alpha \zeta^2$ can indeed be estimated to be in the range of 60 meV. This crude estimate, however, contains a number of uncertainties as field orientation, particle morphology or the exact value of the dielectric response of the quantum dot which could easily change the result by more than one order of magnitude.

Another explanation for the origin of the multiple bands might be the recombination of biexcitons and/or luminescence of higher excited one-pair states. The evolution of multiple luminescence bands at high excitation intensities has been investigated by Wind *et al.* for CdSe nanocrystals.²¹ Besides the well known $1S_{3/2}^h-1S^e$ transition, i.e., the transition from the lowest excited state, two more transitions at higher transition energies and another transition at lower energies have been observed. The band at lower energies was attributed to the recombination of two-pair-states and those at higher energies were attributed to

$2S_{3/2}^h-1S^e$ recombination and higher excited two-pair-states. In fact, a similar model could also explain the single CdS-nanocrystal spectra as the spacing between the distinct transitions and the number of bands do not vary randomly from dot to dot. The reproducible evolution of the small peak at higher energies, which can be clearly seen for both nanocrystals in Fig. 2, was already reported in our first paper.¹⁶ Contradictory to the work of Wind *et al.* we attributed this transition to biexcitonic emission according to Ref. 22.

So far it remains an open question which mechanism could explain the observed features. The intensity fluctuations seen on the left hand side of Fig. 3 suggest that the radiation channels for one single dot switch on a time scale of seconds which favors the surface model. On the other hand, there seems to be no direct correlation between total fluorescence intensity and spectral position such that the luminescence could still come from defined intrinsic electronic states. Extended theoretical work including calculations of the dielectric response of nanoscopic materials and energy levels of two-pair states is needed to explain the fluorescence features of the CdS quantum dots.

IV. COMPARISON OF SINGLE CdS NANOCRYSTALS WITH SINGLE CdS/HgS QDQW's

As can be seen from Fig. 4 the fluorescence spectra and fluorescence time traces of the QDQW's are totally different

as compared to the CdS particles. The spectra were taken at $T=10$ K upon irradiation with $\lambda=633$ nm. While the CdS spectra change dramatically upon increasing laser power the CdS/HgS spectra do not fluctuate at all and a well resolved phonon progression can be observed in all spectra. At the same time the fluorescence time traces show much less intensity fluctuations. The noisy appearance of the upper time trace in Fig. 4 as compared to the data in Fig. 3 is due to a higher time resolution for the QDQW measurements and a lower fluorescence intensity. For the QDQW system besides intensity dependent measurements ($0.02\text{--}50$ kW/cm²) we also performed experiments between 1.4 and 50 K and used different excitation wavelengths (442 nm, 520 nm, 633 nm). None of these measurements showed a remarkable effect on the fluorescence spectra and fluorescence time traces.

The phonon side bands reflect the coupling of the electronic transition to the ionic lattice via ‘‘Froehlich-type’’ interaction. The observed frequency of 285 (± 5) cm⁻¹ is the same as was recently extracted from a detailed analysis of line narrowed fluorescence spectra (FLN) of an ensemble of nanocrystals.²³ The Huang-Rhys-parameter, i.e., the coupling strength was found to be 0.25 (± 0.05) and was calculated from the intensity ratio of the zero- to the one-phonon line. It is a remarkable result that the emission frequency is much closer to the LO-phonon frequency of bulk CdS (300 cm⁻¹) (Ref. 24) than bulk HgS (250 cm⁻¹) (Ref. 25) whereas the phonon frequency in absorption is almost identical to the HgS mode, which has been shown by hole burning experiments.²³ These results strongly support a model in which the ground state phonon frequency is different from the excited state frequency. Using the phonon frequency as a ‘‘ruler’’ for localization it seems that the QDQW ground state is delocalized over the whole nanocrystal whereas the excited state charge carriers are localized in the HgS quantum well. Very recently ultrafast experiments have been performed which support this model.²⁶

Comparing Figs. 3 and 4 it is obvious that the embedding of just one monolayer of HgS changes the spectra dramatically as the charge carriers are eventually confined in the small HgS region of the QDQW. From effective mass calculations it was shown that the probability of presence for the electrons and holes should be more than 50% in the HgS region.¹² This effect would strongly reduce the polarizability of the whole particle thus reducing spectral diffusion processes produced by charge carriers in surface traps. In addition, the outermost CdS layer acts as a tunneling barrier for the charges which reduces the probability of trapping. Stark effect measurements on the QDQW system could verify this assumption.

There is another issue which has to be addressed here and which relates to the ‘‘homogeneous’’ fluorescence spectrum as extracted from previous FLN experiments in comparison to the single dot emission spectrum. In order to derive a ‘‘homogeneous’’ emission spectrum from the measured FLN data a fitting or deconvolution procedure had to be used.²³ In this process a broad unstructured and redshifted fluorescence component was needed in addition to a ‘‘theoretical’’ single particle spectrum to reproduce the FLN data. Basically, in any ensemble fluorescence measurement on CdS (Ref. 7) and CdS/HgS/CdS (Ref. 11) dots, a broad unstructured fluorescence band was observed which was attributed to ‘‘trapped

luminescence.’’ From these ensemble measurements it was argued that the trapped- and the band-edge luminescence might come from the same nanocrystal emitting at different radiation channels.²⁷ In the single dot experiments presented here the particles either show the defined ‘‘band-edge fluorescence’’ as can be seen in the Fig. 4 or the broad unstructured ‘‘trapped’’ luminescence. Sometimes the broad feature evolves for single particles after they have been investigated for a long time at high excitation intensities. These results suggest that the broad fluorescence at longer wavelength stems from imperfect crystallites with, e.g., oxidized surfaces which can either be formed already during preparation or via light irradiation (photooxidation).

V. HIGH RESOLUTION SPECTRA

The width of the CdS and CdS/HgS fluorescence line strongly depends on the excitation intensity as can be seen in Fig. 5. Spectrum (I) in Fig. 5(a) (bold line, hollow spheres) stems from a single CdS nanocrystal excited with 125 W/cm² which results in a full width at half maximum (FWHM) of 10 meV. The spectra (II) and (III) were recorded at 7.5 W/cm² (thin line, solid spheres) and 13 W/cm² (dotted line), respectively. Obviously the linewidth can be reduced dramatically at lower laser intensity which has already been demonstrated for CdSe particles.¹⁵ In addition we could observe an influence of the measured FWHM on acquisition time which can be seen by comparing the spectra (II) and (III) in Fig. 5(a). The excitation intensity of these two spectra is on the same order of magnitude and the spectra were recorded back to back but the center wavelength is shifted by 1.7 meV. This type of spectral diffusion appears to be different from the observation of the various spectral lines discussed in Sec. III, where the separation of the luminescence lines was more than 50 meV. The spectral diffusion shown here leads to a broadening of each fluorescence line as a function of acquisition time and could be due to slight changes in the dot environment. This broadening mechanism is strongly reduced for the QDQW's. For lowest excitation intensities and very long acquisition times we measured linewidth on the order of 1 meV for CdS nanocrystals and less than 0.5 meV for the QDQW's as can be seen in Fig. 5(b).

Especially for the CdS/HgS QDQW's where the line broadening due to spontaneous spectral diffusion is reduced, a strong asymmetry of the fluorescence line can be observed. A similar line shape has been found in a number of inorganic and organic materials^{28,29} and is commonly described as ‘‘Urbach rule’’ behavior. Different theories about this line shape were reported in the early 1970s and the effect was either explained by a coupling of excitons to acoustic modes through the deformation potential of local lattice distortion³⁰ or by exciton ionization via electric microfields.³¹ The electric microfield theory was developed for bulk materials, in which impurities or long wavelength LO phonons larger than the exciton dimensions were discussed to be sources for the ionization. As the investigated nanocrystals are in the range of or smaller than the bulk exciton, we favor the model of thermally excited acoustic phonons to be responsible for the asymmetric luminescence tails. As the quantum yield is not unity obviously not all the energy deposited in the nanocrystal by photoexcitation is converted into fluorescence light. At

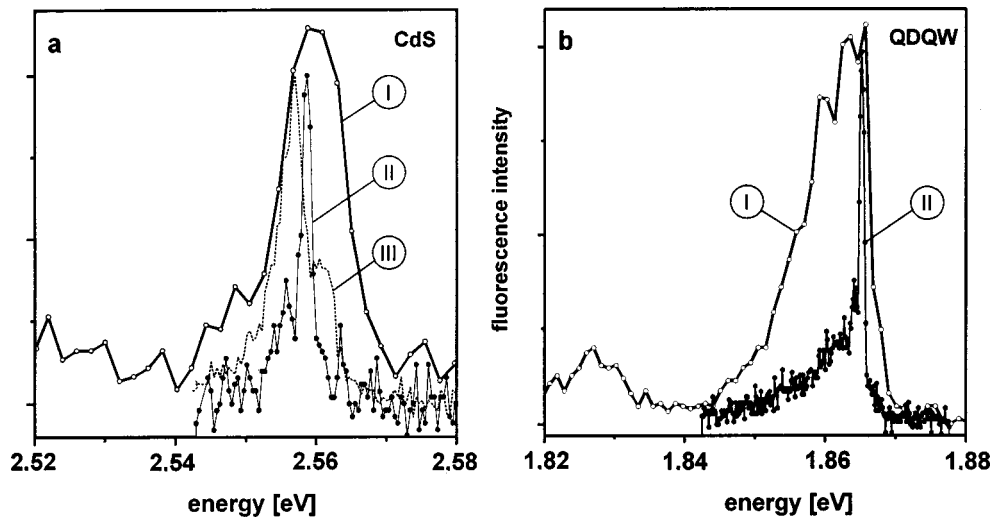


FIG. 5. High resolution fluorescence spectra of single CdS particles [(a) $T=20$ K, $\lambda_{\text{ex}}=442$ nm] and single CdS/HgS/CdS QDQW's [(b) $T=10$ K, $\lambda_{\text{ex}}=633$ nm]. The CdS spectra were recorded at an excitation intensity of 126 W/cm² for 120 s [(I) bold line, hollow spheres], 7.5 W/cm², 600 s [(II) thin line, solid spheres], and 13 W/cm², 600 s [(III) dotted line]. The linewidth can be reduced to approximately 1.5 meV at very low excitation intensity. The shift of the spectra at lowest excitation intensity which were recorded back to back show that the linewidth also depends on the acquisition time. The QDQW spectra show much narrower lines at low excitation intensity: The spectrum recorded at 246 W/cm², 120 s [(I) bold line, hollow spheres] can be narrowed down to less than 0.5 meV at 6 W/cm², 1800 s [(II) thin line, solid spheres]. The spectra clearly show an asymmetric tail towards lower energies.

high excitation intensities the lack of temperature equilibration might result in a heating of the particle and a creation of acoustic lattice vibrations. According to Ref. 30 the tail could then be explained by self trapping of the exciton in energetic levels below the band gap which are produced by these acoustic phonons.

Alivisatos *et al.* have described a formalism to explain the size dependent absorption linewidth of semiconductor nanocrystals via deformation potential coupling which relied heavily on elastic constants of a sphere.³² For the CdS/HgS QDQW's the morphology is very complex and the material constants are not known in all detail. Therefore in a first estimate we used bulk CdS data³³ to calculate the exponential luminescence tails using the "empirical Urbach rule" for different temperatures.³⁰ According to this very preliminary model, the temperature of the investigated QDQW's could exceed a value of several tens already at an excitation intensity of 500 W/cm². This local heating would explain why we could not observe a dependence of the line shape upon excitation at different wavelength or different He-bath temperatures up to 50 K. The results suggest that a study of the genuine line shape can only be done at lowest excitation intensities.

VI. SUMMARY

In this paper we have reported the fluorescence of pure CdS nanocrystals with dimensions in the range of the bulk exciton and of quantum dot quantum wells where one monolayer of HgS is embedded into a CdS nanocrystal. With single dot spectroscopy we could observe pronounced differences in the emission properties which can be explained by a localization of the excited charge carriers within the nanocrystal upon embedding just one monolayer of HgS.

For the CdS nanocrystals up to five transitions could be observed at high excitation intensity ($I > 1$ kW/cm²) where

the reason for the different emission channels is not clear yet. In a first model, charge carriers in surface traps might be responsible for the different transition frequencies by creating an internal Stark effect. In accordance with the huge polarizability of the nanocrystal ($\approx 10^5$ Å³) single charges on opposite sides of a CdS tetrahedron could lead to the different transition frequencies. The measured intensity fluctuations between these transitions on a time scale of seconds support this model. For CdS/HgS/CdS on the other hand, frequency jumps are not present even at highest laser power. This result supports the assumption that the charge carriers are indeed localized within the nanocrystal thus reducing the polarizability and the frequency shifts produced by electric microfields if created at all in these particles. In addition there is much less probability for the charge carriers to tunnel through the passivating outer CdS layers. In a second model, the different transition frequencies for the CdS nanocrystals could come from higher excited one- or two-pair states. Along these lines the QDQW's would behave differently because the strong quantization in the HgS well would lead to energetic levels which are much more separated than those of the CdS nanocrystals whose dimensions are already in the range of the bulk exciton.^{34,35} In any case the emission spectra of the QDQW's consist of discrete transitions and a well resolved phonon progression (285 cm⁻¹) with a frequency close to the CdS LO phonon (300 cm⁻¹). The coupling of the emission to CdS-like phonons suggests that the ground state of the QDQW's is delocalized over the whole particle.

At lowest excitation intensity the linewidth of the nanocrystal emission can be reduced to less than 1 meV. For the CdS nanocrystals the linewidth is determined by spontaneous spectral diffusion and therefore strongly depending on the acquisition time. For the QDQW's where the spectral diffusion processes are strongly reduced we could observe an asymmetric line broadening to the low-energy side upon increasing excitation intensity. This effect could be explained

by acoustic phonons created through nonradiative relaxation of the excitation energy which might be responsible for potential fluctuations thus producing localized states below the delocalized exciton level.

Extended theoretical work is needed to explain the different electronic transition frequencies and the nature of the ground state. The results of effective mass calculations, however, strongly depend on the input parameters (Luttinger parameters, spin-orbit splitting, etc.)³⁶ which are still uncertain especially for cubic CdS and HgS.³⁴ Therefore tight binding

calculations where different particle morphologies and surface effects could be considered as well might be very helpful to understanding the optical properties of the CdS/HgS nanocrystals.

ACKNOWLEDGMENTS

We would like to acknowledge U. Wannek for stimulating discussions and W. Goehde for technical support concerning SPM software and electronics.

*Author to whom correspondence should be addressed.

- ¹H. Weller, *Angew. Chem.* **105**, 43 (1993).
- ²A. P. Alivisatos, *J. Phys. Chem.* **100**, 13226 (1996).
- ³D. J. Norris and M. G. Bawendi, *Phys. Rev. B* **53**, 16 338 (1996).
- ⁴U. Banin, C. J. Lee, A. A. Guzelian, A. V. Kadavanich, A. P. Alivisatos, W. Jakolski, G. W. Bryant, Al. L. Efros, and M. Rosen, *J. Chem. Phys.* **109**, 2306 (1998).
- ⁵H. Fu, L. W. Wang, and A. Zunger, *Phys. Rev. B* **57**, 9971 (1998).
- ⁶J. E. Bowen-Katari, V. L. Colvin, and A. P. Alivisatos, *J. Phys. Chem.* **98**, 4109 (1994).
- ⁷L. Spanhel, M. Haase, H. Weller, and A. Henglein, *J. Am. Chem. Soc.* **109**, 5649 (1987).
- ⁸A. Hässelbarth, A. Eychmüller, R. Eichberger, M. Giersig, A. Mews, and H. Weller, *J. Phys. Chem.* **97**, 5333 (1993).
- ⁹M. A. Hines and P. Guyot-Sionnest, *J. Phys. Chem.* **100**, 468 (1996).
- ¹⁰X. Peng, M. C. Schlamp, A. V. Kadavanich, and A. P. Alivisatos, *J. Am. Chem. Soc.* **119**, 7019 (1997).
- ¹¹A. Mews and A. Eychmüller, *Ber. Bunsenges. Phys. Chem.* **102**, 1343 (1998).
- ¹²D. Schooss, A. Mews, A. Eychmüller, and H. Weller, *Phys. Rev. B* **49**, 17 072 (1994).
- ¹³M. Nirmal, B. O. Dabbousi, M. G. Bawendi, J. J. Macklin, J. K. Trautman, T. D. Harris, and L. E. Brus, *Nature (London)* **383**, 802 (1996).
- ¹⁴S. A. Blanton, M. A. Hines, and P. Guyot-Sionnest, *Appl. Phys. Lett.* **69**, 3905 (1996).
- ¹⁵S. A. Empedocles, D. J. Norris, and M. G. Bawendi, *Phys. Rev. Lett.* **77**, 3873 (1996).
- ¹⁶J. Tittel, W. Göhde, F. Koberling, T. Basché, A. Kornowski, H. Weller, and A. Eychmüller, *J. Phys. Chem. B* **101**, 3013 (1997).
- ¹⁷S. A. Empedocles and M. G. Bawendi, *Science* **278**, 2114 (1997).
- ¹⁸A. Mews, A. Eychmüller, M. Giersig, D. Schooss, and H. Weller, *J. Phys. Chem.* **98**, 934 (1994).
- ¹⁹W. Göhde, J. Tittel, Th. Basché, C. Bräuchle, U. C. Fischer, and H. Fuchs, *Rev. Sci. Instrum.* **68**, 2466 (1997).
- ²⁰A. Mews, A. V. Kadavanich, U. Banin, and A. P. Alivisatos, *Phys. Rev. B* **53**, R13 242 (1996).
- ²¹O. Wind, F. Gindele, U. Woggon, and C. Klingshirm, *J. Cryst. Growth* **159**, 867 (1996).
- ²²Al. L. Efros and A. V. Rodina, *Solid State Commun.* **72**, 645 (1989).
- ²³A. Mews, U. Banin, A. V. Kadavanich, and A. P. Alivisatos, *Ber. Bunsenges. Phys. Chem.* **101**, 1621 (1997).
- ²⁴R. Broser and M. Rosenzweig, in *Numerical Data and Functional Relationships in Science & Technology*, edited by O. Madelung, Landolt-Bornstein, New Series, Group III Vol. 17, Pt. b (Springer-Verlag, Berlin, 1982).
- ²⁵W. Szuskiewicz, K. Dybko, E. Dynowska, J. Górecka, B. Witkowska, B. Hennion, M. Jouanne, and C. Julien, *Acta Phys. Pol.* **92**, 1029 (1997).
- ²⁶A. T. Yeh, G. Cerullo, U. Banin, A. Mews, A. P. Alivisatos, and C. V. Shank, *Phys. Rev. B* **59**, 4973 (1999).
- ²⁷A. Hässelbarth, A. Eychmüller, and H. Weller, *Chem. Phys. Lett.* **203**, 271 (1993).
- ²⁸H. Sumi and Y. Toyozawa, *J. Phys. Soc. Jpn.* **31**, 342 (1971).
- ²⁹A. H. Francis and R. Kopelman, in *Laser Spectroscopy of Solids*, 2nd ed., edited by W. M. Yen and P. M. Selzer, Topics in Applied Physics, Vol. 49 (Springer-Verlag, Berlin, 1986), p. 241.
- ³⁰H. Sumi, *J. Phys. Soc. Jpn.* **32**, 616 (1972).
- ³¹J. D. Dow and D. Redfield, *Phys. Rev. B* **5**, 594 (1972).
- ³²A. P. Alivisatos, A. L. Harris, N. J. Levinos, M. L. Steigerwald, and L. E. Brus, *J. Chem. Phys.* **89**, 4001 (1988).
- ³³F. Spiegelberg, E. Gutsche, and J. Voigt, *Phys. Status Solidi B* **77**, 233 (1976).
- ³⁴W. Jaskolski and G. W. Bryant, *Phys. Rev. B* **57**, R4237 (1998).
- ³⁵K. Chang and J. B. Xia, *Phys. Rev. B* **57**, 9780 (1998).
- ³⁶T. Richard, P. Lefebvre, H. Mathieu, and J. Allegre, *Phys. Rev. B* **53**, 7287 (1995).